DEVELOPMENTAL BIOLOGY **181,** 186–196 (1997)
ARTICLE NO. DB968440

Targeted Mutations in *Hoxa-9* and *Hoxb-9* Reveal Synergistic Interactions

Feng Chen and Mario R. Capecchi[1]

Department of Human Genetics, Howard Hughes Medical Institute, University of Utah School of Medicine, Salt Lake City, Utah 84112

Mice were generated with a targeted disruption of the homeobox-containing gene *hoxb-9*. Mice homozygous for this mutation show defects in the development of the first and second ribs. In most cases the first and second ribs are fused near the point at which the first and second pairs of ribs normally attach to the sternum. Abnormalities of the sternum accompany the rib fusions. These include abnormal attachment of the ribs to the sternum, a reduction in the number of intercostal segments of the sternum, and abnormal growth of the intercostal segments. Over half of the homozygous mutants, as well as some heterozygotes, also have an eighth rib attached to the sternum. These results show that *hoxb-9* plays a significant role in the specification of thoracic skeletal elements. To reveal potential interactions between the paralogous *Hox* genes *hoxa-9* and *hoxb-9,* mice heterozygous for both mutations were intercrossed. Mice homozygous for both mutations show more severe phenotypes than predicted by the addition of the individual mutant phenotypes. Both the penetrance and the expressivity of the rib and sternal defects are increased, suggesting synergistic interactions between these genes. In particular, the sternum defects are greatly exacerbated. Interestingly, the defects in *hoxb-9* and *hoxa-9/hoxb-9* mutant mice are concentrated along the axial column at points of transition between vertebral types.

INTRODUCTION

Hox genes encode transcription factors belonging to the *Antennapedia* homeodomain class. The mammalian *Hox* complex contains 39 genes distributed on 4 linkage groups designated as HoxA, B, C, and D. This organization is believed to have arisen early in vertebrate phylogeny by quadruplication of an ancestral complex common to vertebrates and invertebrates (Pendleton *et al.,* 1993; Holland and Garcia-Fernandez, 1996). Based on DNA sequence and the position of the genes on their respective chromosomes, individual members of the 4 linkage groups have been classified into 13 paralogous families. Members of a paralogous family often share similar gene expression patterns.

In *Drosophila* the homologous genes (*Hom C* genes) are used to pattern the developing embryo along its rostrocaudal axis (Akam, 1987; Gehring, 1987). Mutations in some of these genes change the identity of one parasegment into that of a neighboring parasegment (Lewis, 1978). Mutational analysis in the mouse has demonstrated that the *Hox* genes, alone or in concert with other *Hox* genes, are also used to regionalize the embyo along its major body axes (Chisaka and Capecchi, 1991; Lufkin *et al.,* 1991; Chisaka *et al.,* 1992; LeMouellic *et al.,* 1992; Condie and Capecchi, 1993; Dollé *et al.,* 1993; Gendron-Maguire *et al.,* 1993; Jeannotte *et al.,* 1993; Ramirez-Solis *et al.,* 1993; Rijli *et al.,* 1993; Small and Potter, 1993; Davis and Capecchi, 1994; Kostic and Capecchi, 1994; Satokata *et al.,* 1995; Suemori *et al.,* 1995; Boulet and Capecchi, 1996; Goddard *et al.,* 1996). Thus mutations in the 3′ *Hox* genes affect the formation of anterior structures whereas disruption of 5′ genes gives rise to posterior abnormalities. Regionalization of the embryo by *Hox* genes appears to be accomplished by the controlled temporal and spatial activation of these genes such that a 3′ gene is activated prior to and in a more anterior region of the embryo than its 5′ neighbor (Duboule and Dollé, 1989; Graham *et al.,* 1989; Duboule, 1994; Capecchi, 1997). However, *Hox* genes function as components of highly integrated circuits such that paralogous genes, adjacent genes on the same linkage group, and even nonparalogous genes in separate linkage groups interact positively, negatively, and in parallel with each other to orchestrate the morphological regionalization of the embryo (Condie and Capecchi, 1994; Rancourt *et al.,* 1995; Davis *et al.,* 1995; Horan *et al.,* 1995a, b; Barrow and Capecchi, 1996; Davis and Capecchi, 1996; Favier *et al.,* 1996; Fromental-Ramain *et al.,* 1996).

[1] To whom correspondence should be addressed.

0012-1606/97 $25.00

AID DB 8440 / 6x15$$$141 12-27-96 23:34:55 dba

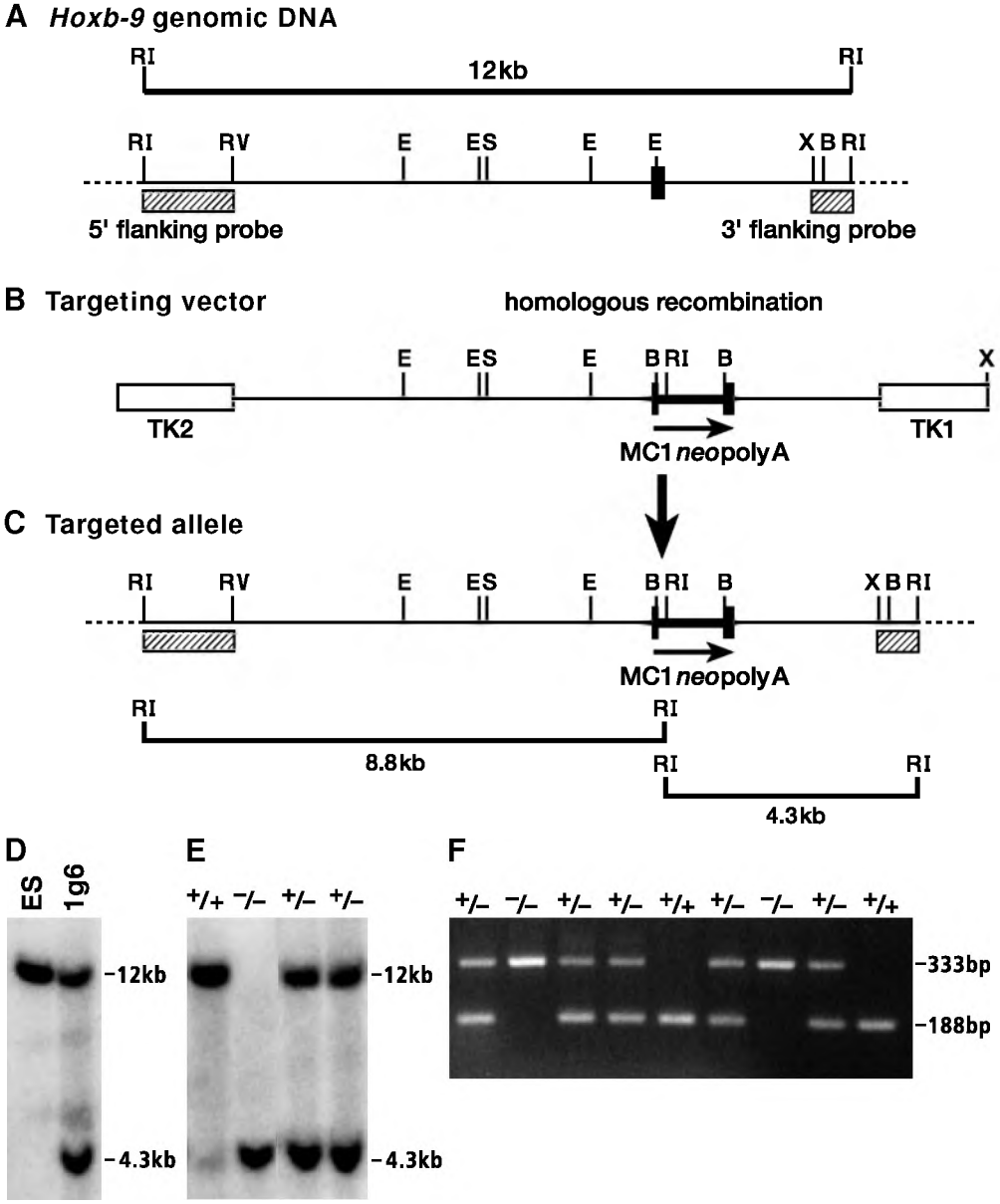

FIG. 1. Disruption of the *hoxb-9* gene and analysis of the mutant genotype. (A–C) Diagrams of the wild-type *hoxb-9* locus, the targeting vector, and the targeted allele, respectively. The black box indicates the homeobox of *hoxb-9*. *Hoxb-9* is transcribed from left to right. The bars indicate restriction fragments produced by *Eco*RI digest. RI, *Eco*RI; RV, *Eco*RV; E, *Eco*47III; S, *Sal*I; X, *Xho*I; B, *Bam*HI. (D, E) Southern transfer analyses of the targeted cell line and of the intercross genotypes, respectively. Genomic DNA was digested with *Eco*RI and probed with the 3′ flanking probe. The 12- and 4.3-kb bands were from the wild-type and mutant alleles, respectively. (F) PCR analysis of the intercross genotypes. The wild-type band is 188 bp and the mutant band is 333 bp.

Although all 39 *Hox* genes are likely to be involved in the formation of the axial skeleton, the specific malformations caused by mutations in individual *Hox* genes are difficult to predict. Some of this difficulty can be attributed to overlap of function between genes of the same paralogous group or between genes of different paralogous groups. The rostrocaudal direction of apparent homeotic transformations of vertebrae seen in *Hox* mutants is also unpredictable. In fact, the two polarities can appear in the same mutant (Jeannotte *et al.*, 1993; Small and Potter, 1993). Often the defects are observed at the anterior limit of the *Hox* gene expression pattern, a phenomenon that has led to the proposal of the

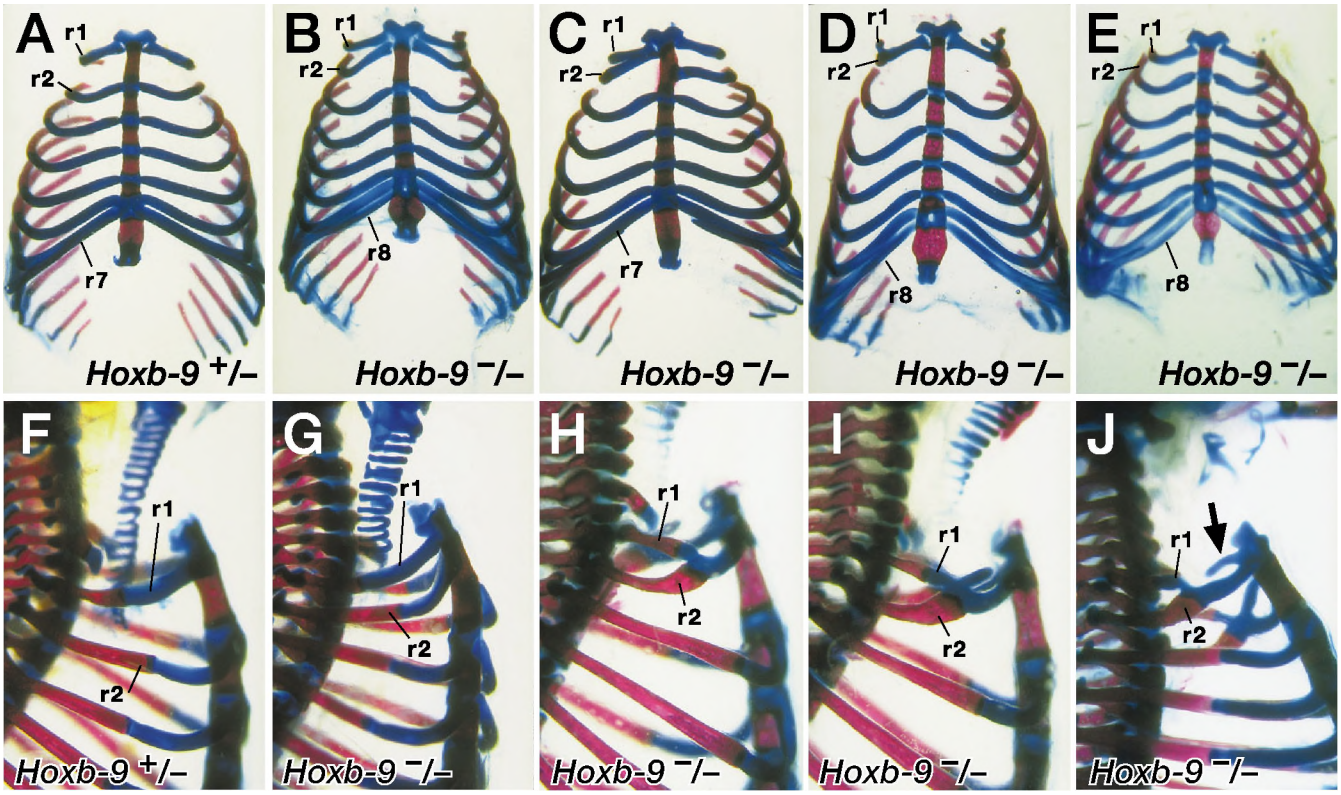

FIG. 2. Defects in the thoracic skeleton in *hoxb-9*−/− mice. (A–E) Ventral views of the thoracic skeletons with the vertebral columns removed. (F–J) Lateral views of the upper thoracic regions of the same embryos showing different types of first and second rib fusions. The black arrow points to a ventral rib element which connects only to the sternum.

posterior prevalence model (Duboule, 1991). However, even this correlation has many exceptions. A model that, in its broad sense, is likely to be correct is that the combination of *Hox* genes expressed in a given region determines the identity of structures in that region. However, such combinatorial models should not be viewed as a code involving simple addition of elements, because these gene products, as already pointed out, are likely to interact positively, negatively, and in parallel with each other. Simple combinatorial models based on overlapping *Hox* gene expression patterns have in fact been woefully inaccurate in predicting vertebral identities. Instead, the interactions among *Hox* genes are sufficiently complex that their role in specifying the vertebral column must be functionally determined on a case by case basis through analyses of both individual and appropriate combinations of *Hox* gene mutations.

Herein we describe the phenotypic consequences of disrupting *hoxb-9* in mice, as well as the effects of combining *hoxb-9* and *hoxa-9* mutations. These mice show defects in the formation of the thoracic skeleton.

TABLE 1
Skeletal Phenotypes in Mice Deficient for *hoxb-9*

Phenotypes	+/+ (n = 11)	+/− (n = 27)	−/− (n = 24)
First and second rib fusion	0	0	20 (83%)
Bilateral	0	0	18
Unilateral	0	0	2
Articulating eighth rib	0	2 (7.4%)	13 (54%)
Both sides	0	2	12
One side	0	0	1

MATERIALS AND METHODS

Targeting Vector

A 9.9-kb genomic clone containing the *hoxb-9* gene was isolated from a λ DNA library prepared from mouse CC1.2 embryo-derived stem (ES) cells and used to construct a replacement-type targeting

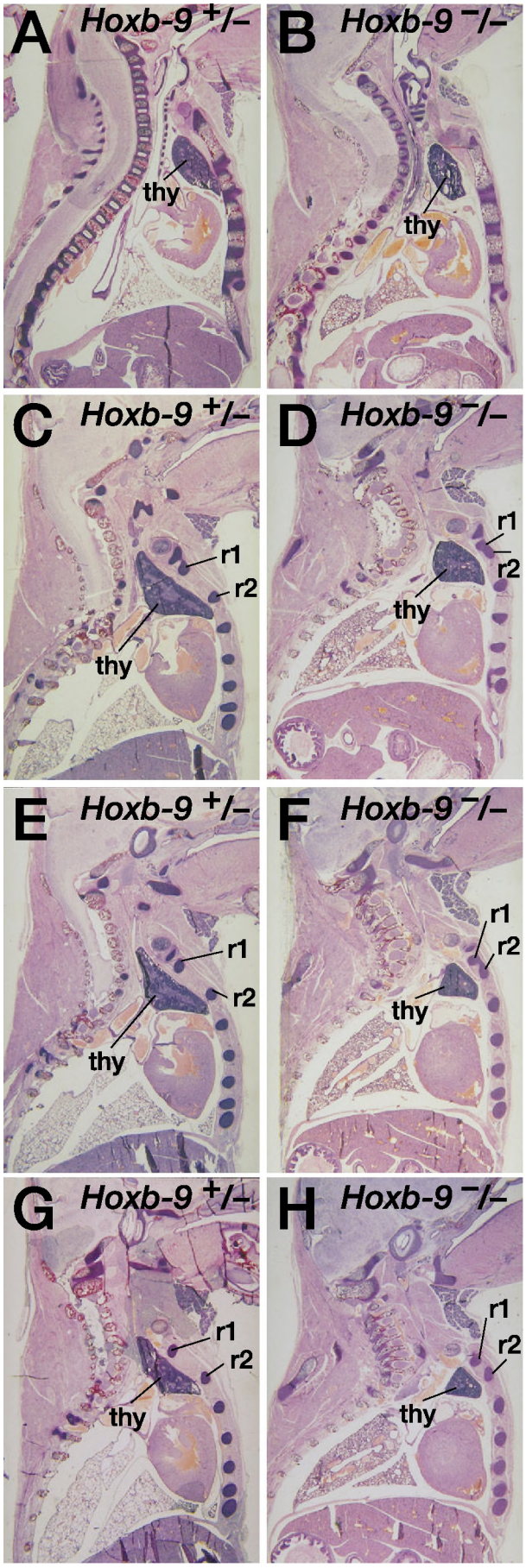

vector. In order to disrupt the *hoxb-9* coding sequence, the MC1*neo* poly(A) cassette (Thomas and Capecchi, 1987) was inserted into the *Eco*47III site within the homeodomain. Completion of the targeting vector involved flanking the *hoxb-9* genomic sequences with the HSV1 and HSV2 thymidine kinase genes (Fig. 1).

Electroporation and the Generation of hoxb-9 Mutant Mice

The targeting vector was linearized by digestion with *Xho*I and electroporated into R1 ES cells (Deng and Capecchi, 1992; Nagy *et al.*, 1993). ES cells containing a disruption of the *hoxb-9* gene were enriched by positive–negative selection (Mansour *et al.*, 1988). DNA samples isolated from colonies of ES cells were digested with *Eco*RI and probed with 5′ and 3′ flanking probes (Fig. 1). Two percent of the ES cell lines contained the desired *hoxb-9* mutation. The targeted ES cell line (1g6) was used to generate chimeric mice that transmitted the *hoxb-9* mutant allele to their progeny (Capecchi, 1989, 1994).

The Generation of Mice Deficient for Both hoxa-9 and hoxb-9

The *hoxa-9* mutant mice used in this study were generated by Peterson, Chisaka, and Capecchi (unpublished data). Since both *hoxa-9*−/− mice and *hoxb-9*−/− mice are fertile (Fromental-Ramain *et al.*, 1996), compound heterozygotes for *hoxa-9* and *hoxb-9* mutations (*hoxa-9*+/− and *hoxb-9*+/−) were obtained from crosses between these homozygous mutant mice.

Genotype Analysis

DNA was prepared from tail biopsies of adult and newborn mice and from yolk sacs of embryos. *Hoxb-9* genotypes were determined either by Southern transfer analysis with the 3′ flanking probe or by amplification of DNA fragments using the polymerase chain reaction (PCR). *Hoxa-9* genotypes were determined by PCR. The sequences of the PCR primers used for this analysis were: *hoxb-9* forward primer, 5′CTCCAATGCCAGGGGAGTAG3′; *hoxb-9* reverse primer, 5′CTTCTCTAGCTCCAGCGTCTGG3′; MC1*neo* reverse primer for *hoxb-9*, 5′GTGTTCGAATTCGCCAATGACAAG3′; *hoxa-9* forward primer, 5′CGCTGGAACTGGAGAAGGAGTTTCTG3′; *hoxa-9* reverse primer, ATCCTGCGGTTCTGGAACCAGATC3′; MC1*neo* reverse primer for *hoxa-9*, 5′TCTATCGCCTTCTTGACGAGTTC3′. An example of the *hoxb-9* genotyping results is given in Fig. 1.

Histology

Newborn mice were euthanized by asphyxiation with CO_2, fixed in 4% formaldehyde in phosphate-buffered saline (PBS) overnight

FIG. 3. Sagittal sections of *hoxb-9*+/− and −/− newborn mice. Sections (A) and (B), (C) and (D), (E) and (F), (G) and (H) were from similar positions of the mice. Sections from top to bottom were taken progressively further away from the midlines of the mice. The space in the upper thoracic region and the size of the thymus are reduced in the *hoxb-9*−/− mutants with rib fusions.

at room temperature (Manley and Capecchi, 1995), and embedded in paraffin according to standard protocols. Ten-micrometer serial sagittal sections were collected and regressively stained with hematoxylin and eosin (Chisaka and Capecchi, 1991). Newborn and adult whole mount skeletons were prepared as described by Mansour *et al.* (1993).

Whole Mount in Situ Hybridization

Whole mount *in situ* hybridization on E9.0–E12.5 embryos was performed as described (Carpenter *et al.*, 1993; Manley and Capecchi, 1995). The concentration of digoxigenin–UTP-labeled RNA probes in the hybridization mixture was approximately 0.4 μg/ml. Alkaline phosphatase-conjugated anti-digoxigenin Fab fragment was used at a 1:4000 dilution. The templates for *hoxb-9*, *hoxb-8*, and *hoxb-7* RNA *in situ* probes were as follows: a 517-bp fragment in the 3′ untranslated region (UTR) of *hoxb-9*, a 356-bp *Sac*I–*Kpn*I fragment from the 3′ UTR of *hoxb-8*, and a 524-bp fragment from the 3′ UTR of *hoxb-7*, respectively.

RESULTS

Generation of hoxb-9 Mutant Mice

The structure of the targeting vector used to disrupt the *hoxb-9* gene in R1 ES cells is shown in Fig. 1. The insertion of the *neo* cassette into the *hoxb-9* homeobox terminates the protein prior to all three helixes of the homeodomain and therefore should render the gene product nonfunctional with respect to DNA binding. Southern transfer analyses, using 5′ and 3′ probes flanking the targeting vector as well as an internal probe, were used to ensure that no rearrangements of the *hoxb-9* locus had occurred other than the desired *neo* insertion into the homeodomain. A representative targeted cell line was used to produce chimeric males that passed the *hoxb-9* mutation through the germline.

Hoxb-9 Mutants Are Viable and Fertile

Mice heterozygous for the *hoxb-9* mutation were intercrossed to produce homozygotes. Adult *hoxb-9−/−* mice were obtained at a frequency predicted from a Mendelian distribution of mutant and wild-type alleles, indicating no loss of mutant alleles as a consequence of embryonic or postnatal lethality. *Hoxb-9−/−* mice appear outwardly normal and animals of both sexes are fertile.

Hoxb-9 Mutant Mice Display Skeletal Defects in the Thoracic Region

The skeletons of *hoxb-9* mutant mice showed malformations in the thoracic region (Table 1, Fig. 2). Of 24 *hoxb-9−* homozygotes examined, 20 had fusions of the first and second ribs. Ninety percent of the fusions were bilateral.

The sternum of a normal mouse consists of six ossified segments, the manubrium, four sternebrae, and the xiphoid process. In animals with first and second rib fusions on both sides of the body, the normal cartilage centers associated with the attachment of the second pair of ribs are absent (Fig. 2). As a result, the upper sternum has one less ossified segment. The absence of that ossified segment causes the upper rib cage to be shortened by approximately 35% in the distance from the manubrium to the point where the third rib articulates with the sternum. This shortening is in part due to the loss of two growth plates normally present at the ends of each ossified segment. Segmentation of the sternum results from the attachment of the ribs to the sternum which locally inhibits the hypertrophy of the cartilaginous cells of the sternum near the attachment site (Chen, 1953). Thus, the observed abnormal segmentation patterns of the sternum can be understood in terms of the abnormal patterns of first and second rib attachment to the sternum.

The majority of the first and second rib fusions occurred at the point of attachment with the sternum (Fig. 2G). About 25% of the fusions occurred by alternative pathways. For example, in some animals the first and second ribs fused prior to attachment to the sternum, formed a common ventral rib, and then attached to the sternum (Fig. 2H). In other mutants, the first rib branched after fusion. In some of these cases both branches were articulated with the sternum; in others only one branch was attached. Finally, in two homozygotes the first rib attached to the sternum but lost connection with either the second rib or the dorsal portion of the first rib, implicating remodeling after first rib attachment (Fig. 2J).

Thirteen of the 24 *hoxb-9−/−* mice examined had an eighth rib attached to the sternum on one or both sides (Figs. 2B, 2D, and 2E). A similar phenotype has been described in *hoxc-8* and *hoxc-9* mutant mice (LeMouellic *et al.*, 1993; Suemori *et al.*, 1995). Such eighth rib attachment appears to occur independently of the first and second rib fusions, since some animals had eighth rib articulations with the sternum but did not show first and second rib fusions (Fig. 2E). Approximately 7% of the *hoxb-9−* heterozygotes also showed eighth rib attachment to the sternum. This phenotype was never observed in wild-type control animals. The thoracic vertebral bodies of *hoxb-9−/−* mice appear normal. Thus, the defects appear to be restricted to the patterning of the ribs and sternum (i.e., the ventral aspects of the thoracic axial column). Formation of the appendicular axis appears normal in *hoxb-9* mutant homozygotes.

Histological Examination of hoxb-9−/− Mice

Sagittal and parasagittal sections of newborn *hoxb-9* homozygous mutant mice reveal a significant reduction in the size and an alteration in the shape of the thymus relative to wild-type and *hoxb-9* heterozygous littermates (Fig. 3). The cortex and medulla of the thymus in *hoxb-9−/−* mice, however, appear normal. We presume that the altered shape of the thymus is an indirect effect of the reduced space in the upper thoracic region in *hoxb-9* mutant homozygotes. Consistent with this hypothesis, *hoxb-9* expression is not observed in tissues contributing to the formation of thymus.

AID DB 8440 / 6x15$$$142 12-27-96 23:34:55 dba

TABLE 2

Thymus Weight Comparison between *hoxb-9* Homozygous Mutants with and without the First and Second Rib Fusions[a]

Genotype	With rib fusion	Thymus weight "*T*" (g)	Body weight "*B*" (g)	T/B[b]
−/−	Yes	0.022	3.9	0.0056
−/−	No	0.024	3.6	0.0067
−/−	No	0.027	4.2	0.0064
−/−	Yes[c]	0.026	4.4	0.0060
−/−	Yes	0.022	4.5	0.0049
−/−	Yes	0.026	4.5	0.0058
−/−	Yes	0.021	4.2	0.0050

Note. Thymus weight was independently normalized to heart weight and the results were indistinguishable from those shown above.

[a] These are 8-day-old littermates from a cross between two *hoxb-9* homozygous mutants.

[b] If we use $T/B_{f,a}$ for the average value of T/B for mutants with the rib fusions (Nos. 1, 4, 5, 6, and 7), we get $T/B_{f,a} \approx 0.0055$; if we use $T/B_{n,a}$ for the average value of T/B for mutants without the rib fusions (Nos. 2 and 3), we get $T/B_{n,a} \approx 0.0066$. The difference between these two values is 20%.

[c] No. 4 had rib fusions that were not as severe as the other rib fusions observed in this litter.

Also, mutant animals do not appear to be compromised with respect to their immune function. For example, fluorescence–cytometric analysis of blood from mutant and control mice showed a normal distribution of T and B lymphocytes (data not shown). Finally, as previously mentioned, the rib fusions which are responsible for the reduction in the size of the upper thoracic cavity are not present in all *hoxb-9* mutant homozygotes. When the weight of excised thymic tissues was compared between *hoxb-9* mutant homozygous mice with and without the first and second rib fusions, the average ratio of thymus to body mass in mutants with the rib fusions was 20% lower than in mutants with normal ribs (Table 2).

E13.5 embryos were immunostained with the 2H3 antibody directed against a subunit of the neurofilament protein (Dodd *et al.,* 1988) to reveal possible changes in the pattern of neurons in the peripheral nervous system. No neuronal defects were apparent in *hoxb-9* mutant homozygotes either in the body wall or in the limbs (data not shown).

Hoxb-9 Is Expressed at the Axial Level from Which Affected Skeletal Elements Arise

The defects in the upper thoracic region of *hoxb-9*− homozygotes are found at significantly more rostral levels than the reported anterior limits of expression for *hoxb-9* or its paralogues at E12.5 (Bogarad *et al.,* 1989; Burke *et al.,* 1995). To resolve this discrepancy, we reexamined the expression of *hoxb-9* at E9.5, E10.5, E11.5, and E12.5 using whole mount RNA *in situ* hybridization (Fig. 4). In E9.5 embryos, the expression of *hoxb-9* was strong in the neural tube with an anterior limit at the level of somites 7–8 (pV3). At this time, a high level of expression in the somites was detected in the posterior portion of the embryo but lower levels were seen in the rostral portion of the embryo. Expression in the somites could, however, be readily detected up to the level of the seventh to eighth somite. At E10.5, the anterior limit of expression in the neural tube shifted rostrally by one to two somites. Expression in the spinal ganglia was also apparent. Paraxial mesoderm expression appeared to be enhanced in ventral portions of the somites. At E11.5 and E12.5, changes in neural tube expression were not apparent. However, the intensity of the RNA hybridization signal decreased progressively in the anterior region of the embryos in paraxial mesoderm-derived structures which included the vertebral bodies and rib primordia. *Hoxb-9* expression was evident in the kidneys from E12.5 onward.

From these studies, it is evident that at E9.5, the anterior limit of *hoxb-9* expression is sufficiently anterior to cover the region of thoracic defects observed in *hoxb-9* mutant mice. The anterior limit of expression in paraxial mesoderm-derived structures then shifts caudally. However, *hoxb-9* expression is apparent in the regions of the rib and sternum primordia (i.e., the tissues affected by the *hoxb-9* mutation).

The hoxb-9 Mutation Does Not Affect the Expression of Neighboring Hox Genes

It has been reported that in some cases a mutation in one *Hox* gene can affect the expression of a neighboring *Hox* gene (Suemori *et al.,* 1995; Barrow and Capecchi, 1996; Boulet and Capecchi, 1996). To determine if the *hoxb-9* mutation affected *hoxb-8* or *hoxb-7* expression, we conducted whole mount RNA *in situ* hybridization experiments on E10.5 and E12.5 embryos of all three *hoxb-9* genotypes (i.e., +/+; +/−; −/−). Neither the anterior limits of *hoxb-8* expression in the neural tube or in paraxial mesoderm-derived structures nor the overall level of *hoxb-8* expression was distinguishable in embryos of these three *hoxb-9* genotypes (Fig. 5). Similarly, the expression pattern of *hoxb-7* was not affected in *hoxb-9* heterozygous and mutant homozygous embryos (data not shown). Thus, neither the presence of the *neo* insertion in *hoxb-9* nor the absence of functional *hoxb-9* protein appears to affect the expression of the neighboring *Hox* genes.

As a further test for relationships between *hoxb-9* and neighboring *Hox* genes, *hoxb-9/hoxb-8* and *hoxb-9/hoxb-7* transheterozygotes were constructed by crossing *hoxb-9* mutants with *hoxb-8* (Greer and Capecchi, data not shown) or *hoxb-7* (Chen and Capecchi, unpublished data) mutants. At low frequencies (20%), *hoxb-9/hoxb-7* transheterozygotes (i.e., *hoxb-9*+/−; *hoxb-7*−/+ mice) and (14%) of *hoxb-9/hoxb-8* transheterozygotes showed first and second rib fusions very similar to those observed in *hoxb-9*− homozygotes. Such fused ribs have never been observed in mice heterozygous for *hoxb-9, hoxb-8,* or *hoxb-7* alone. Such non-

allelic noncomplementation suggests that *hoxb-7, hoxb-8,* and *hoxb-9* gene products directly or indirectly interact to specify the upper thoracic region of the mouse (Rancourt *et al.,* 1995).

Hoxa-9/hoxb-9 Double Mutants

Hoxa-9 mutant mice have been described by Fromental-Ramain *et al.* (1996). Since both *hoxa-9−/−* and *hoxb-9−/−* mice are fertile, compound heterozygotes for both *hoxa-9* and *hoxb-9* could be obtained from crosses between *hoxa-9* and *hoxb-9* mutant homozygotes. These compound heterozygotes appeared outwardly normal and were fertile. Mice of all nine possible genotypes were obtained from crosses between such compound heterozygotes, and the nine genotypes were obtained at the expected Mendelian ratios, indicating that all genotypes, including double mutant homozygotes, were viable.

Skeletal Defects in hoxa-9/hoxb-9 Double Mutants

Hoxa-9 mutant homozygotes have an extra pair of fully grown ribs on the 21st vertebra (i.e., show an anterior homeosis of the 1st lumbar vertebra to a thoracic vertebra; Fromental-Ramain *et al.,* 1996). *Hoxa-9* heterozygotes occasionally have small rib anlage on the 1st lumbar vertebra (Peterson, Chisaka and Capecchi, unpublished results). *Hoxa-9* heterozygotes carrying one or two mutant alleles of *hoxb-9* had a pair of full-size 14th ribs (Table 3, Fig. 6). Thirty-eight percent of *hoxa-9+/−*, *hoxb-9+/−* mice had pairs of fully grown ribs. The penetrance increased to 53% in *hoxa-9+/−*; *hoxb-9−/−* mice, indicating a quantitative effect of the *hoxb-9* mutant alleles on mediation of this homeosis in mice heterozygous for the *hoxa-9* mutation. An increase in the penetrance of the 1st and 2nd rib fusion phenotype was also observed when *hoxb-9* homozygous mutant mice received one or two copies of the *hoxa-9* mutant allele (Table 3 and Fig. 6). Approximately 83% of *hoxb-9* homozygous mice show 1st and 2nd rib fusions (Table 1), while 93% of the *hoxa-9+/−*; *hoxb-9−/−* mice and 100% of the *hoxa-9−/−*; *hoxb-9−/−* mice show rib fusions. Moreover, the rib fusions in *hoxa-9/hoxb-9* double mutants are more severe. Some double mutants even had the 3rd rib fused to the 1st and 2nd rib fusion (Fig. 6). Exacerbation of sternum defects is also evident in the *hoxa-9/hoxb-9* double mutants (Fig. 6H). In such animals the length of all of the intercostal segments is greatly reduced. As is evident from Figs. 6F, 6G, and 6H, the expressivity of the sternum defects varies in the *hoxa-9/hoxb-9* double mutants, suggesting that other members of this paralogous family may play important roles in patterning the thoracic vertebrae. The more severe abnormalities evident in *hoxa-9−/−*; *hoxb-9−/−* mice compared to defects observed in *hoxa-9* and *hoxb-9* single mutant homozygotes support the hypothesis that these two genes function synergistically to pattern the thoracic vertebrae.

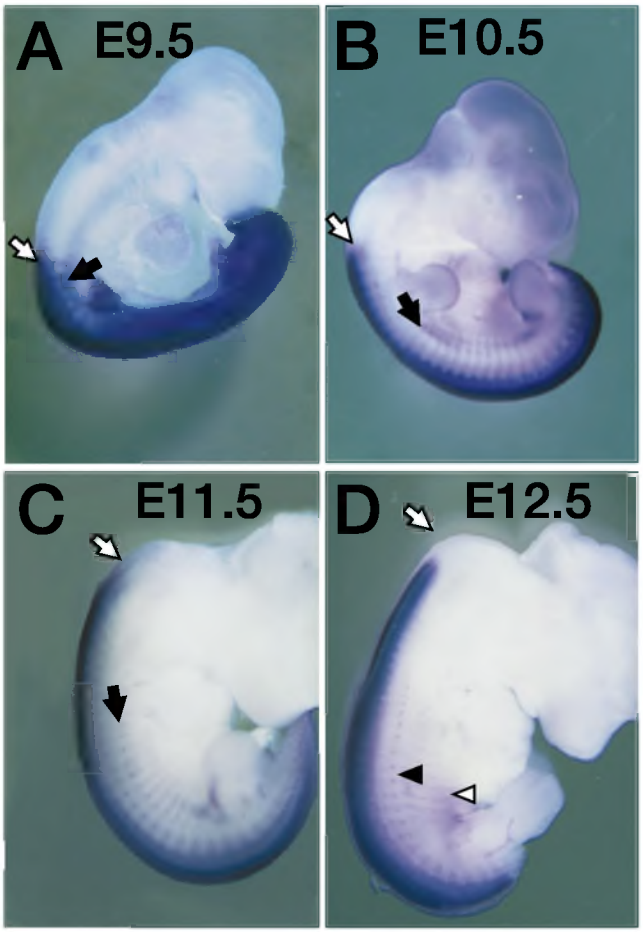

FIG. 4. The expression of *hoxb-9* in wild-type embryos. The anterior limit of neural tube expression (white arrow) and the anterior limit of paraxial mesoderm expression (black arrow) are at approximately pV3 at E9.5 (A). The anterior limit of neural tube expression shifts rostrally by one to two somites at E10.5 (B) and remains unchanged at E11.5 (C) and E12.5 (D). The anterior limit of paraxial mesoderm expression shifts caudally in the upper thoracic region between E9.5 and E10.5. The intensity of the signal from mesoderm expression decreases progressively and becomes restricted to structures that appear to be primordia of the vertebral bodies (black triangle) and ribs (white triangle).

DISCUSSION

Eighty-three percent of the *hoxb-9* homozygous mutants examined had first and second rib fusions while 54% of homozygotes and a small number of heterozygotes showed abnormal attachment of the eighth rib to the sternum. Both of these defects can be interpreted in terms of anterior homeotic transformations. In many *hoxb-9* mutant homozygotes, the articulation angle and position of sternal attachment of the second rib resembles those of the first rib. Normally, the first rib has two attachment points with the

AID DB 8440 / 6x15$$$143 12-27-96 23:34:55 dba

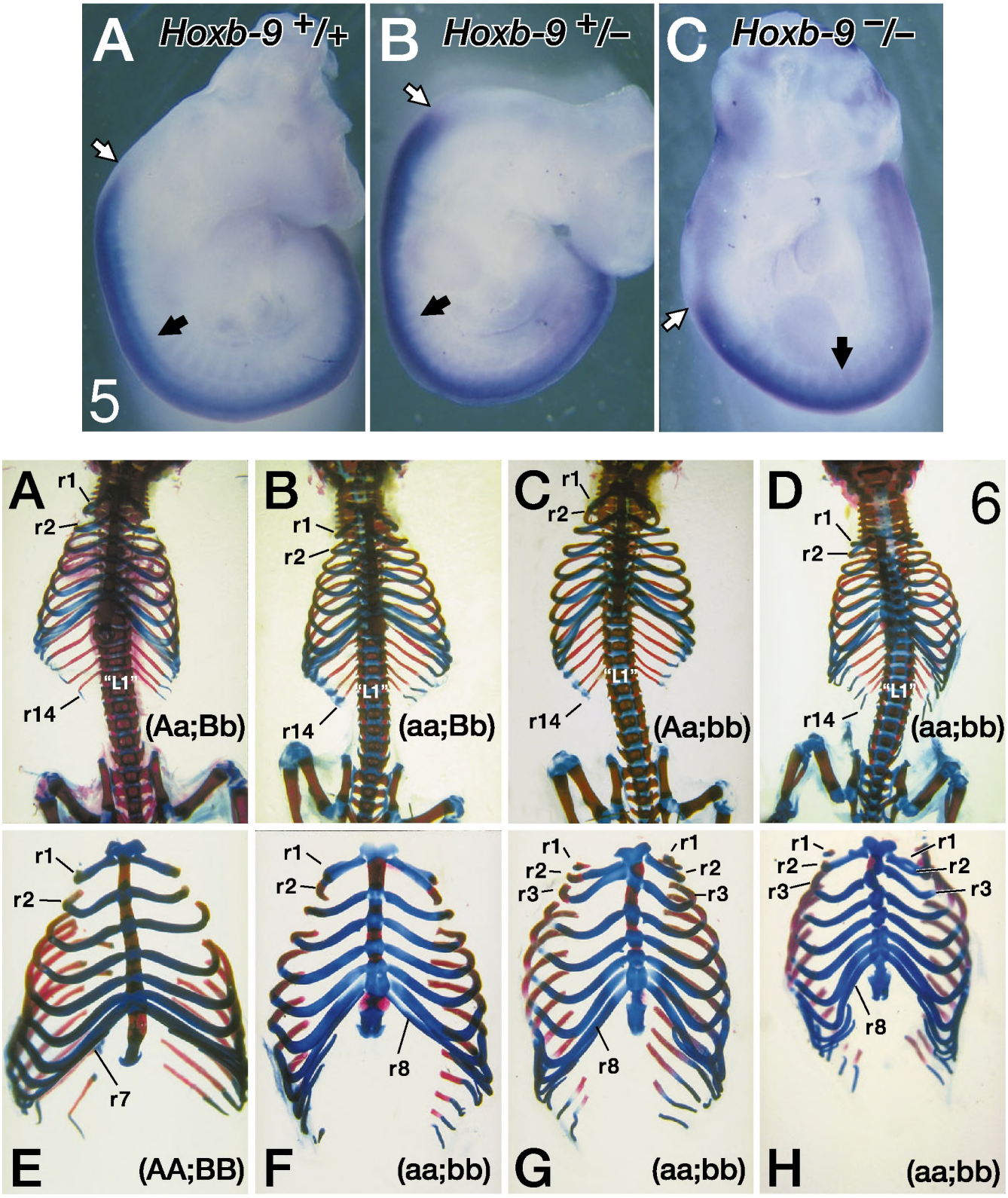

FIG. 5. The expression pattern of *hoxb-8* does not change in *hoxb-9* mutants. (A) *hoxb-9*+/+, (B) *hoxb-9*+/−, (C) *hoxb-9*−/−. White arrows indicate the anterior limits of neural tube expression. Black arrows indicate the anterior limits of mesoderm expression.

AID DB 8440 / 6x15$$8440 12-27-96 23:34:55 dba

TABLE 3
Summary of Skeletal Phenotypes in (*hoxa-9; hoxb-9*) Mice

Phenotypes	Aa;Bb (n = 16)[a]	aa;Bb (n = 11)	Aa;bb (n = 15)	aa;bb (n = 9)
First and second rib fusion	0	0	14 (93%)	9 (100%)[b]
Articulating eighth rib	1 (6%)	1 (9%)	8 (53%)	5 (56%)
14 pairs of ribs	6 (38%)	11 (100%)	8 (53%)	9 (100%)

[a] A, *hoxa-9* wild-type allele; a, *hoxa-9* mutant allele; B, *hoxb-9* wild-type allele; b, *hoxb-9* mutant allele;
[b] Three (aa;bb) mice had the third rib fused to the second rib. When this happened, the T1 ribs either fused to the T2 ribs or lost contact with the sternum and any other ribs.

sternum: one at the tip of the manubrium, the other at the body of the manubrium. The other ribs have only one point of articulation. In mice with the first and second rib fusions, the second rib tends to have two attachment points that resemble those of the first rib. The abnormal attachment of the eighth rib to the sternum can also be regarded as the eighth rib acquiring seventh rib character, since in the mutant it morphologically resembles the seventh rib.

The formation of the sternum is also abnormal in *hoxb-9* mutant homozygotes. However, it is not clear whether these defects are a direct consequence of the *hoxb-9* mutation or the consequence of aberrant articulations with defective ribs. Segmentation of the sternum clearly results from articulation with the ribs (Chen, 1952). Further, defective segmentation would also be expected to alter the growth of the sternebrae. Thus, the fact that we observe sternum defects in the upper thoracic region of *hoxb-9* mutant homozygotes can be understood either in terms of defective rib patterning or in terms of a direct role of *hoxb-9* in sternum formation. However, the more extensive sternum defects observed in *hoxa-9/hoxb-9* double mutants support the second hypothesis. In most of the *hoxa-9/hoxb-9* double mutants, the entire sternum is hypoplastic and malformed. Such extensive sternum malformations are not readily interpreted as resulting solely from the defects in the articulations of the first, second, or eighth ribs, but instead suggest an additional role for *hoxa-9* and *hoxb-9* in sternum formation. This is an important distinction since ribs and sternum originate from separate mesodermal lineages.

It is curious that in *hoxb-9* mutant homozygotes, defects are observed in the formation of the first, second, and eighth ribs with intervening ribs appearing normal. However, closer examination indicates that the angle of articulation of the ribs with the sternum is abnormal along the entire ribcage (Fig. 2). This indicates that the *hoxb-9* mutation contributes to mispatterning of the ribs, and possibly the sternum, from T1 through T8, with the defects only being more apparent at the ends of this block of vertebrae.

A consequence of the rib fusions seen in some *hoxb-9* mutant mice is a reduction in the size of the upper thoracic cavity. Interestingly, in those *hoxb-9* mutant homozygotes that have first and second rib fusions, the size of the thymus is also reduced. The reduction in the size of the thymus appears to result as a secondary response to the reduction in the size of the upper thoracic cavity since in *hoxb-9* mutant mice lacking rib fusions the thymus is normal in size. These observations suggest that the size of the thymus is regulated with respect to the size of the thoracic cavity.

Hoxa-9/hoxb-9 Double Mutants

Mice homozygous for mutations in either *hoxa-9* and *hoxb-9* do not show overlapping phenotypes. Yet double mutants show exacerbation of all of the defects observed in either *hoxa-9*− or *hoxb-9*− homozygotes. In addition, both the penetrance and expressivity of the defects correlate with the number of mutant alleles present in the mouse. For example, mice heterozygous for either the *hoxa-9* or the *hoxb-9* mutation never show full-size 14th ribs. However, such ribs are apparent in some *hoxa-9, hoxb-9* compound heterozygous mice and the frequency is increased in *hoxa-9+/−, hoxb-9−/−* mice. Conversely, *hoxa-9−/−* mice have never been observed to have 1st and 2nd rib fusions. However, the frequency of such fusions in *hoxb-9−/−* mice progressively increases with the addition of one and then two *hoxa-9* mutant alleles. Similar observations have been made in mice containing combinations of *hoxa-3* and *hoxd-3* mutant alleles (Condie and Capecchi, 1994). These observations again emphasize the extensive quantitative interactions among *Hox* genes required to specify the vertebrate body plan. Each *Hox* gene appears to have individual unique functions as well as more extensive roles in combination

FIG. 6. Skeletal defects in the *hoxa-9/hoxb-9* mutant mice. (A–D) Skeletal defects in mice with four combinations of *hoxa-9* and *hoxb-9* mutant alleles (see text for details). (E–H) Alterations in the thoracic skeleton in *hoxa-9−/−, hoxb-9−/−* mice. Various rib fusions, abnormal rib attachments to the sternum, and general malformations of the sternum are apparent. Genotype symbols: A, *hoxa-9* wild-type allele; a, *hoxa-9* mutant allele; B, *hoxb-9* wild-type allele; b, *hoxb-9* mutant allele. "L1" indicates the first lumbar vertebra which bears ribs.

with other *Hox* genes. The concentration of *Hox* gene products in different cells must be very tightly regulated since the reduction of *Hox* protein concentration in heterozygotes can result in marked phenotypic consequences.

Genetic interactions between *hoxa-9* and *hoxd-9* have been reported (Fromental-Ramain *et al.,* 1996). In this case, the interactions are observed in more caudal aspects of the vertebral column compared to those seen in *hoxa-9/hoxb-9* double mutants. Specifically, Fromental-Ramain *et al.* (1996) observed in mice mutant for both *hoxa-9* and *hoxd-9* an exacerbation of defects in the lumbosacral axial skeleton. Thus, the domain of influence of *hoxa-9* extends from the first thoracic vertebra, when interacting with *hoxb-9,* to sacral vertebrae, when interacting with *hoxd-9.*

As the functions of increasing numbers of *Hox* genes are unraveled, patterns are emerging. With respect to the formation of the axial column, there appear to be hot spots for the accumulation of defects. Such defects are particularly evident at the boundaries between changes in vertebral type, such as the base of the skull and the first cervical vertebra, C7 and T1, T7 and T8, T13 and L1, L6 and S1, and S4 and Ca1. For example, mutations in *hoxb-2, hoxb-4, hoxd-1, hoxd-3,* and *hoxd-4* show defects in the formation of the first cervical vertebra, the atlas (Barrow and Capecchi, 1996; Ramirez-Solis *et al.,* 1993; Condie and Capecchi, 1993; Horan *et al.,* 1995a, b). Mutations in *hoxa-4, hoxa-5, hoxa-6, hoxb-5, hoxb-6, hoxb-7, hoxb-8,* and *hoxb-9* have defects in C7, T1, or both and so on. Why is this the case? Part of the answer is operational. It is very apparent when C7 acquires ectopic ribs or T1 loses ribs. On the other hand, transformations of C5 to C4 are more difficult to score. Second, we can anticipate that the generation of the major morphological differences associated with the different vertebral classes will require the concerted activity of more *Hox* genes than the generation of the smaller differences within a vertebral class. Finally, the vertebral classes may be formed as units using prescribed developmental programs. Consistent with this hypothesis, the expression patterns of *Hox* genes in the prevertebrae of the chick and mouse maintain register with the type of vertebrae rather than the position of the vertebra along the axial column (Burke *et al.,* 1995). In mice in which the continuity of the normal program has been disrupted by a *Hox* mutation, the discontinuities in the specification of cells are likely to be most apparent at the transitions between vertebral types, making such boundaries particularly vulnerable to dysmorphology.

ACKNOWLEDGMENTS

We especially acknowledge Osamu Chisaka for cloning the *hoxb-9* mouse genomic sequences and for preparing the *hoxb-9* targeting vector. We thank M. Allen, C. Lenz, G. Peterson, S. Barnett, E. Nakashima, and M. Wagstaff for excellent technical assistance and L. Oswald for help with preparation of the manuscript.

REFERENCES

Akam, M. E. (1987). The molecular basis for metameric pattern in the *Drosophila* embryo. *Development* **101,** 1–22.

Barrow, J. R., and Capecchi, M. R. (1996). Targeted disruption of the *hoxb-2* locus in mice interferes with expression of *hoxb-1* and *hoxb-4. Development,* **122,** 3817–3828.

Bogarad, L. D., Utset, M. F., Awgulewitsch, A., Miki, T., Hart, C. P., and Ruddle, F. H. (1989). The developmental expression pattern of a new murine homeobox gene: *Hox-2.5. Dev. Biol.* **133,** 537–549.

Boulet, A. M., and Capecchi, M. R. (1996). Targeted disruption of *hoxc-4* causes esophageal defects and vertebral transformations. *Dev. Biol.* **177,** 232–249.

Burke, A. C., Nelson, C. E., Morgan, B. A., and Tabin, C. (1995). *Hox* genes and the evolution of vertebrate axial morphology. *Development* **121,** 333–346.

Capecchi, M. R. (1989). Altering the genome by homologous recombination. *Science* **244,** 1288–1292.

Capecchi, M. R. (1994). Targeted gene replacement. *Sci. Am.* **270,** 52–59.

Capecchi, M. R. (1997). The role of *Hox* genes in hindbrain development. *In* "Molecular and Cellular Aspects of Neural Development" (W. M. Cowan, T. M. Jessell, and S. L. Zipursky, Eds.), Oxford Univ. Press, New York, in press.

Carpenter, E. M., Goddard, J. M., Chisaka, O., Manley, N. R., and Capecchi, M. R. (1993). Loss of *Hox-A1* (*Hox-1.6*) function results in the reorganization of the murine hindbrain. *Development* **118,** 1063–1075.

Chen, J. M. (1952). Studies on the morphogenesis of the mouse sternum I. Normal embryonic development. II. Experiments on the origin of the sternum and its capacity for self-differentiation *in vitro. J. Anat.* **86,** 373–401.

Chen, J. M. (1953). Studies on the morphogenesis of the mouse sternum I. Normal embryonic development. II. Experiments on the closure and segmentation of the sternal bands. *J. Anat.* **87,** 130–149.

Chisaka, O., and Capecchi, M. R. (1991). Regionally restricted developmental defects resulting from targeted disruption of the mouse homeobox gene *hox-1.5. Nature* **350,** 473–479.

Chisaka, O., Musci, T. S., and Capecchi, M. R. (1992). Developmental defects of the ear, cranial nerves and hindbrain resulting from targeted disruption of the mouse homeobox gene *Hox-1.6. Nature* **355,** 516–520.

Condie, B. G., and Capecchi, M. R. (1993). Mice homozygous for a targeted disruption of *Hoxd-3* (*Hox-4.1*) exhibit anterior transformations of the first and second cervical vertebrae, the atlas and the axis. *Development* **119,** 579–595.

Condie, B. G., and Capecchi, M. R. (1994). Mice with targeted disruptions in the paralogous genes *hoxa-3* and *hoxd-3* reveal synergistic interactions. *Nature* **370,** 304–307.

Davis, A. P., and Capecchi, M. R. (1994). Axial homeosis and appendicular skeleton defects in mice with a targeted disruption of *hoxd-11. Development* **120,** 2187–2198.

Davis, A. P., Witte, D. P., Hsieh, L. H., Potter, S. S., and Capecchi, M. R. (1995). Absence of radius and ulna in mice lacking *hoxa-11* and *hoxd-11. Nature* **375,** 791–795.

Davis, A. P., and Capecchi, M. R. (1996). A mutational analysis of the 5′ Hox D genes: Dissection of genetic interactions during limb development in the mouse. *Development* **122,** 1175–1185.

Deng, C., and Capecchi, M. R. (1992). Reexamination of gene targeting frequency as a function of the extent of homology between

the targeting vector and the target locus. *Mol. Cell. Biol.* **12,** 3365–3371.

Dodd, J., Morton, S. B., Karagogeos, D., Yamamoto, M., and Jessell, T. M. (1988). Spatial regulation of axonal glycoprotein expression on subsets of embryonic spinal neurons. *Neuron* **1,** 105–116.

Dollé, P., Dierich, A., Le Meur, M., Schimmang, T., Schuhbaur, B., Chambon, P., and Duboule, D. (1993). Disruption of the *Hoxd-13* gene induces localized heterochrony leading to mice with neotenic limbs. *Cell* **75,** 431–441.

Duboule, D., and Dollé, P. (1989). The structural and functional organization of the murine *Hox* gene family resembles that of *Drosophila* homeotic genes. *EMBO J.* **8,** 1497–1505.

Duboule, D. (1991). Patterning in the vertebral limb. *Curr. Opin. Genet. Dev.* **1,** 211–216.

Duboule, D. (1994). Temporal colinearity and the phylotypic progression: a basis for the stability of a vertebrate Bauplan and the evolution of morphologies through heterochrony. *Development (Suppl.),* 135–142.

Favier, B., Rijli, F. M., Fromental-Ramain, C., Fraulob, V., Chambon, P., and Dollé, P. (1996). Functional cooperation between the non-paralogous genes *Hoxa-10* and *Hoxd-11* in the developing forelimb and axial skeleton. *Development* **122,** 449–460.

Fromental-Ramain, C., Warot, X., Lakkaraju, S., Favier, B., Haack, H., Birling, C., Dierich, A., Dollé, P., and Chambon, P. (1996). Specific and redundant functions of the paralogous *Hoxa-9* and *Hoxd-9* genes in forelimb and axial skeleton patterning. *Development* **122,** 461–472.

Gehring, W. J. (1987). Homeoboxes in the study of development. *Science* **236,** 1245–1252.

Gendron, M. M., Mallo, M., Zhang, M., and Gridley, T. (1993). *Hoxa-2* mutant mice exhibit homeotic transformation of skeletal elements derived from cranial neural crest. *Cell* **75,** 1317–1331.

Goddard, J. M., Rossel, M., Manley, N. R., and Capecchi, M. R. (1996). Mice with targeted disruption of *hoxb-1* fail to form the motor nucleus of the VIIth nerve. *Development,* **122,** 3217–3228.

Graham, A., Papalopulu, N., and Krumlauf, R. (1989). The murine and *Drosophila* homeobox gene complexes have common features of organization and expression. *Cell* **57,** 367–378.

Holland, P. W. H., and Garcia-Fernandez, J. (1996). *Hox* genes and chordate evolution. *Dev. Biol.* **173,** 382–395.

Horan, G. S. B., Ramírez-Solis, R., Featherstone, M. S., Wolgemuth, D. J., Bradley, A., and Behringer, R. R. (1995a). Compound mutants for the paralogous *hoxa-4, hoxb-4,* and *hoxd-4* genes show more complete homeotic transformations and a dose-dependent increase in the number of vertebrae transformed. *Genes Dev.* **9,** 1667–1677.

Horan, G. S. B., Kovacs, E. N., Behringer, R. R., and Featherstone, M. S. (1995b). Mutations in paralogous *Hox* genes result in overlapping homeotic transformations of the axial skeleton: Evidence for unique and redundant function. *Dev. Biol.* **169,** 359–372.

Jeannotte, L., Lemieux, M., Charron, J., Poirier, F., and Robertson, E. J. (1993). Specification of axial identity in the mouse: Role of the *Hoxa-5* (*Hox1.3*) gene. *Genes Dev.* **7,** 2085–2096.

Kostic, D., and Capecchi, M. R. (1994). Targeted disruptions of the murine *hoxa-4* and *hoxa-6* genes result in homeotic transformations of components of the vertebral column. *Mech. Dev.* **46,** 231–247.

Le Mouellic, H., Lallemand, Y., and Brulet, P. (1992). Homeosis in the mouse induced by a null mutation in the *Hox-3.1* gene. *Cell* **69,** 251–264.

Lewis, E. B. (1978). A gene complex controlling segmentation in *Drosophila. Nature* **278,** 565–570.

Lufkin, T., Dierich, A., LeMeur, M., Mark, M., and Chambon, P. (1991). Disruption of the *Hox-1.6* homeobox gene results in defects in a region corresponding to its rostral domain of expression. *Cell* **66,** 1105–1119.

Manley, N. R., and Capecchi, M. R. (1995). The role of *hoxa-3* in mouse thymus and thyroid development. *Development* **121,** 1989–2003.

Mansour, S. L., Thomas, K. R., and Capecchi, M. R. (1988). Disruption of the proto-oncogene *int-2* in mouse embryo-derived stem cells: A general strategy for targeting mutations to non-selectable genes. *Nature* **336,** 348–352.

Nagy, A., Rossant, J., Nagy, R., Abramow-Newerly, W., and Roder, J. C. (1993). Derivation of completely cell culture-derived mice from early-passage stem cells. *Proc. Natl. Acad. Sci. USA* **90,** 8424–8428.

Pendleton, J. W., Nagai, B. K., Murtha, M. T., and Ruddle, F. H. (1993). Expansion of the *Hox* gene family and the evolution of chordates. *Proc. Natl. Acad. Sci. USA* **90,** 6300–6304.

Ramírez-Solis, R., Zheng, H., Whiting, J., Krumlauf, R., and Bradley, A. (1993). *Hoxb-4* (*Hox-2.6*) mutant mice show homeotic transformation of a cervical vertebra and defects in the closure of the sternal rudiments. *Cell* **73,** 279–294.

Rancourt, D. E., Tsuzuki, T., and Capecchi, M. R. (1995). Genetic interaction between *hoxb-5* and *hoxb-6* is revealed by nonallelic noncomplementation. *Genes Dev.* **9,** 108–122.

Rijli, F. M., Mark, M., Lakkaraju, S., Dierich, A., Dollé, P., and Chambon, P. (1993). A homeotic transformation is generated in the rostral branchial region of the head by disruption of *Hoxa-2,* which acts as a selector gene. *Cell* **75,** 1333–1349.

Satokata, I., Benson, G., and Maas, R. (1995). Sexually dimorphic sterility phenotypes in *Hoxa10*-deficient mice. *Nature* **374,** 460–463.

Small, K. M., and Potter, S. S. (1993). Homeotic transformations and limb defects in *Hoxa-11* mutant mice. *Genes Dev.* **7,** 2318–2328.

Suemori, H., Takahashi, N., and Noguchi, S. (1995). *Hoxc-9* mutant mice show anterior transformation of the vertebrae and malformation of the sternum and ribs. *Mech. Dev.* **51,** 265–273.

Thomas, K. R., and Capecchi, M. R. (1987). Site-directed mutagenesis by gene targeting in mouse embryonic-derived stem cells. *Cell* **51,** 503–512.

Received for publication August 20, 1996
Accepted September 21, 1996